TIME-DEPENDENT DEFORMATION AND DAMAGE GROWTH IN A NONLINEAR VISCOELASTIC RUBBER-TOUGHENED FIBER COMPOSITE

Robert T. Bocchieri, Applied Research Associates, Inc., Mountain View, CA

Abstract

The constitutive theory developed by Schapery (1999) is first tailored for a continuous fiber composite to develop a Damage Effect Study which identifies the material parameters affected by damage, thereby separating the damage and stress effects on softening. This method is based on 'vertical shifting' of creep-recovery data at different constant damage states, much like vertical shifting for the effect of stress. It is then implemented on a rubber-toughened carbon/epoxy composite. Several significant simplifications are found for the material studied.

A method of Acoustic Emission monitoring and waveform analysis is also developed as a means for tracking what is believed to be the primary damage mechanisms in these materials, matrix cracking and fiber/matrix debond. With direct monitoring, the extent of damage in the material does not need to be inferred from its effect on the stress-strain response. Unidirectional coupons of the rubber-toughened composite studied are monitored in this way for various loading histories. An interpretation of the AE data is proposed based on an initial population of existing flaws. Then a cumulative distribution function (CDF) of microcracking is defined and used to study effects of stress history.

Introduction

An important durability issue in polymeric composites is their loss in stiffness over time. At the fiber and ply-level, this softening is primarily due to viscoelasticity and viscoplasticity of the polymer matrix and time-dependent damage growth. Damage here refers to all microstructural changes such as matrix cracking, fiber/matrix debonding and shear yielding. A good understanding of this softening behavior and its causes is needed to make reliable predictions of more serious larger-scale damage, such as transverse cracking, which may lead to fiber breakage, delamination and finally catastrophic failure. Indeed, these other damage mechanisms, prior to catastrophic failure, may themselves be 'design-driving' failure modes depending on the application and play a critical role in material durability. In terms of durability, material behavior over long times or many fatigue cycles is needed. Certain material behavior, such as viscoelasticity, may seem negligible over typical time-frames used for tests in the laboratory if standard rate-type loadings are used. However, in the long-term neglected strains may become significant.

Effects of damage in both elastic [(Schapery, 1987),(Schapery, 1990b)] and viscoelastic [(Schapery, 1990a), (Park and Schapery, 1997), (Ha and Schapery, 1997), (Abdel-Tawab and Weitsman, 1998)] composites have been incorporated in constitutive equations with the use of internal state variables to represent microstructural damage. As the polymer matrix is a viscoelastic material, cracking of the matrix between the fibers and at the fiber-matrix interface is time or rate-dependent. These theories have been successfully applied to linearly viscoelastic particle filled elastomers where all nonlinearity is due to damage [(Park and Schapery, 1997),(Ha and Schapery, 1997)]. Abdel-Tawab and Weitsman (1998) applied a uniaxial model, contained in the model proposed by Park and Schapery 1997, to a swirl-mat glass-fiber composite.

When a material contains all possible softening mechanism (i.e. nonlinear viscoelasticity, viscoplasticity and damage) there is no apparent way to isolate the effect of damage and its growth from the other softening effects based solely on stress-strain data because mathematical models for mechanical behavior are too limited at this time. The rate of damage growth itself may depend on the entire loading history in a fashion that needs to be experimentally determine. *The ability to track the state of damage and identify which nonlinear parameters in the constitutive model are affected by damage would greatly simplify the characterization process.*

Herein, a method of modal acoustic emission monitoring and data interpretation (Bocchieri et.al., 2002) is used to track microcracking in a unidirectional rubber-toughened composite when loaded in the off-axis directions with various loading histories. An interpretation of the AE data is proposed leading to a cumulative distribution function of microcracking which is used as a damage variable and to study effects of stress history. A Damage Effect Study is then proposed which identifies the parameters in a nonlinear viscoelastic constitutive model that are affected by damage. These studies are implemented on the rubber-toughened composite under study.

Experimental Arrangements

The material studied was comprised of AS4C carbon fibers with a rubber-toughened epoxy resin E719LT ($V_f = 58\%$). Unidirectional 6-ply plates were cut into 90° , 45° , and 30° off-axis samples (1.27 cm in width) with a diamond grinding wheel to minimize edge damage. Full details on specimen design and testing conditions can be found in [(Bocchieri and Schapery, 2000)(Bocchieri et.al., 2002)].

Damage Effect Study

The Damage Effect Study was designed to take advantage of the data analysis method developed by (Schapery, 1969) for evaluating nonlinear viscoelastic (NLVE) material parameters without growing damage. By conditioning the material at various stress levels and evaluating the conditioned response at the identical stress for each damaged state, one can quickly tell which material parameters are affected by damage. The idea is similar to that of residual strength after fatigue testing (e.g. (Hashin and Rotem, 1978)) except here we are concerned with the time-dependent behavior at each damage state.

Figure 1 shows a generic loading history for conducting a Damage Effect Study. Three damage states are shown,designated by state S_i, having been conditioned at stress σ_i. For this material, it was found that 9 cycles was sufficient for conditioning as the response became repeatable, indicating no significant damage or viscoplastic strain over the time of each additional cycle. Given sufficient additional cycles, as done in fatigue testing, further changes would likely be seen. Duplicate 'conditioned' cycles were performed at each stress, for each damaged state to obtain an average response. In this generic example, the NLVE parameters can be compared at three damage states for stress σ_1 and at two damage states at σ_2. Sufficient time for recovery should be left between conditioning and subsequent cycles so that the rate of change in strain does not affect the subsequent cycle (waiting for complete recovery is not always practical).
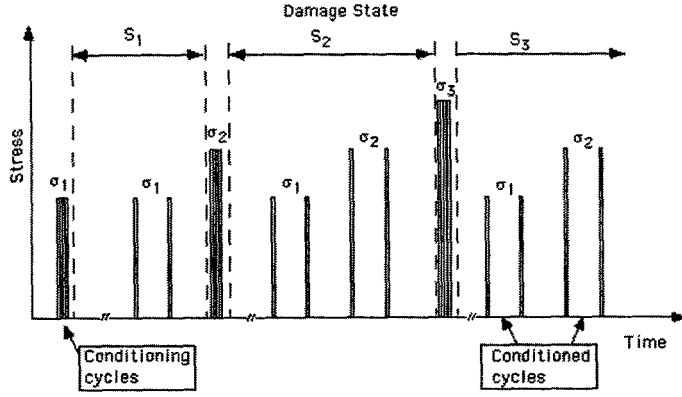
Figure 1. Generic loading history for conducting a damage effect study. Duration of each creep cycle is the same. Three damage states are shown, designated by S_i corresponding to conditioning at σ_i.

Evaluating the Effect of Damage

Analysis of Conditioned Material

If the material is cycled each time for time t_i at stress σ, viscoplastic strain and the growth of damage becomes negligible over the time t_i. When this is the case we will call the material 'conditioned' and having constant damage, S^c. The creep and recovery strains can be written as,

$$\frac{\epsilon_c - \epsilon_{vp}^c}{\sigma} = g_0^c D_0 + \frac{g_1^c g_2^c}{a_\sigma^n} D_1 t^n \tag{1}$$

$$\frac{(\epsilon_r - \epsilon_{vp}^c)}{\sigma t_i^n} = \frac{g_1^{lc} g_2^c}{a_\sigma^n} D_1 [(1 - a_\sigma \lambda)^n - (a_\sigma \lambda)^n]. \tag{2}$$

where, for example,

$$g_0^c = g_0^c(\sigma, S^c) \tag{3}$$

so that g_0^c, g_1^c, g_2^c can take different values for different damage states at the same stress. The ϵ_c and ϵ_r are the creep and recovery strains, ϵ_{vp}^c is the viscoplastic strain, a_σ a scalar function of stress, n a constant and g_1^{lc} is the conditioned low-stress value of g_1. The λ is normalized time

$$\lambda = \frac{t - t_i}{t_i} \tag{4}$$

Derivation of these equations from the constitutive theory proposed in (Schapery, 1999) is fully outlined in (Bocchieri, 2001) and will be the subject of a forthcoming paper.

Damage Effect on Creep

Analysis of creep at different damage states is performed by plotting data versus t^n; n is known from low stress testing. The slope gives $\frac{g_1^c g_2^c D_1}{a_\sigma^n}$ and the intercept $g_0^c D_0$. It has been assumed that a_σ is independent of damage. Comparing creep curves at the same stress, the ratio of the slopes for damage states S_a and S_b is

$$R_c = \frac{g_1^c(S_b) g_2^c(S_b)}{g_1^c(S_a) g_2^c(S_a)}. \tag{5}$$

The ratio of the intercepts is,

$$R_e = \frac{g_0^c(S_b)}{g_0^c(S_a)}. \tag{6}$$

3

Damage Effect on Recovery

The effect of damage on recovery can be evaluated by plotting the recovery data on a log-log scale similar to evaluating the effect of stress (Schapery, 1969). From Equation 2,

$$log\left(\frac{\epsilon_r - \epsilon_{vp}^c}{\sigma t_i^n}\right) = log(g_1^{lc}g_2^c) + log\left(\frac{D_1}{a_\sigma^n}\right) + log[(1 - a_\sigma\lambda)^n - (a_\sigma\lambda)^n]. \qquad (7)$$

If, indeed, the effect of damage is only in $g_1^{lc}g_2^c$, data at different damage states can be vertically shifted to coincide. With a negligible damage effect on the linear behavior g_1^{lc} becomes unity and the ratio of this shift is

$$R_r = \frac{g_2^c(S_b)}{g_2^c(S_a)}. \qquad (8)$$

The effect of damage on g_1^{lc} can be found from low stress testing at each damage state where ($g_2^c = a_\sigma = 1$). However, it was found that the small change in this parameter was approximately the same for all stresses considered and can therefore be neglected in evaluating the higher stress response ($g_1^l c = 1.08$ in 90° samples and 1.0 in off-axis samples).

Comparison of the Damage Effect on Creep and Recovery

Evaluating R_c, R_e, R_r at different damage levels can immediately yield meaningful conclusions:

1. If the effect of damage is only the vertical shift of Equation 7 $\Rightarrow a_\sigma$ is independent of damage.

With a_σ independent of damage:

1. If $R_r = R_c \Rightarrow g_1^c$ is independent of damage.

2. If $R_e = 1 \Rightarrow g_0^c$ is independent of damage. The elastic response is not affected.

Even if changes in g_1^{lc} with damage state are not negligible, R_r can be adjusted for this change and the first comparison still made.

Results from the Damage Effect Study

The Damage Effect Study was performed on 30° , 45° off-axis and 90° unidirectional samples for a total of three combinations of the primary ply stresses. Following is a sample study performed on a 30° sample. Results from the 90° and 45° samples yield the same general conclusions about the material parameters (Bocchieri, 2001). A stress-strain curve with the conditioning stresses used are shown for reference in Figure 2.

Figure 3 shows the effect of damage on the *shear* creep and recovery compliances at 38 and 59 MPa. Each curve represents the average of multiple cycles and displayed good repeatability. Note that the recovery curves have been vertically shifted to the lowest damage state, indicating that damage does *not* affect the function a_σ. It should also be noted that a small amount of constant strain, which is not a plastic strain, has been removed. This strain is most likely an effect of the two phases of material mentioned in the discussion on microcracking. Analyses of these data as previously discussed yields the damage ratios shown in Figure 4. Here we have defined the damage state, S, as the value of the Cumulative Distribution Function of microcracking presented in the section on the analysis of distributed microcracking. At both stress levels, the creep and recovery ratios, R_c and R_r, are *not* the same. This indicates that damage affects *both* g_2^c and g_1^c. *Transverse* creep and recovery data were similar to the shear data. However, as shown in Figure 4, the creep and recovery ratios, R_c and R_r, are the same, indicating that damage
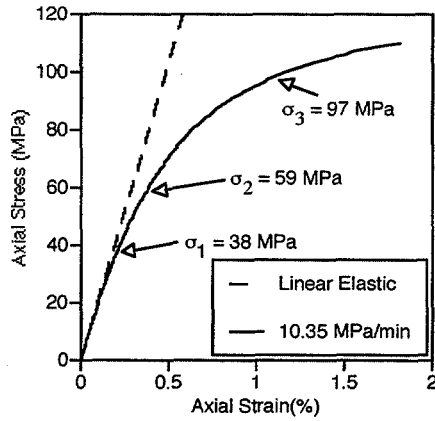
4

Figure 2. Stress strain response of 30° samples with the stresses used in the damage effect study.
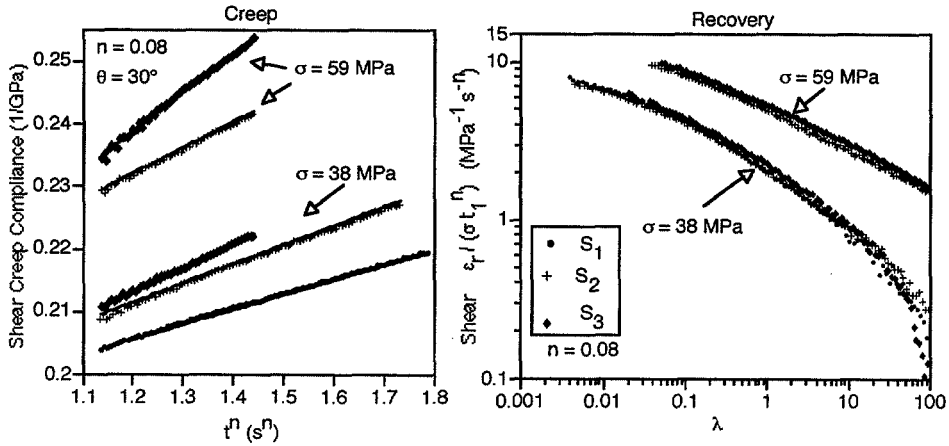

Figure 3. Shear creep compliance of a 30° off-axis sample at 38 MPa and 59 MPa for three damage states. Damage states S_1 and S_2 were cycled 9 times for 100s at each stress. Damage state S_3 is from a single 100s cycle.

does *not* affect g_1^c. Both elastic compliances stiffen slightly with increased damage as R_e decreases with S.

## Modal Acoustic Emission Monitoring of Microcracking

The objective of this AE study was to develop a method of monitoring microcracks directly so that damage evolution equations can be developed. Previously, such equations have been developed based on the implied effect of microdamage on stress-strain response. In an independent microscopy study by Wood and Bradley(1997) on the same carbon/epoxy in this study, it was found that matrix cracking and fiber/matrix debonding were the mechanisms of damage viewed in this material when loaded off-axis to the fibers. They found a variety of initial flaws in the material prior to loading, including voids, cracks around voids and fiber/matrix debonds that initiated this cracking. Only acoustic signals originating from these damage mechanisms were accepted by locating events using two sensors and progressively eliminating all other possible mechanisms that may cause acoustic signals (Bocchieri et.al., 2002).

5
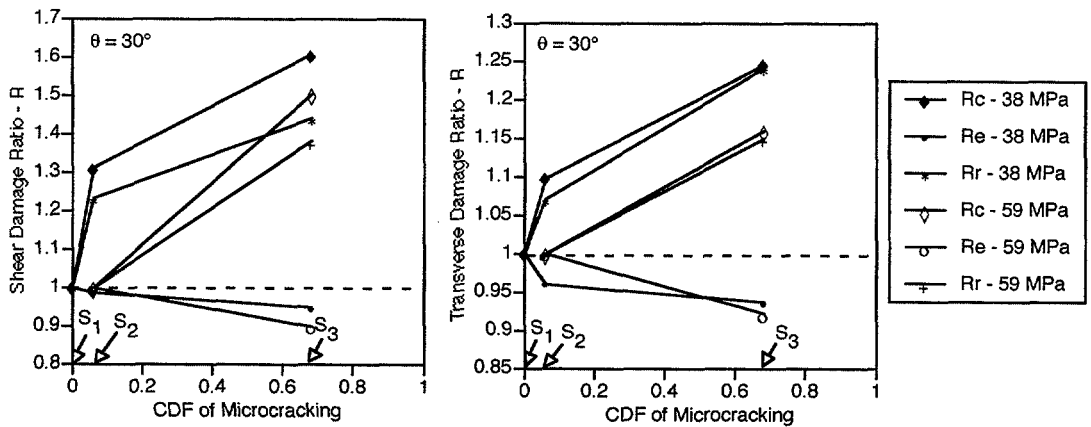
Figure 4. Shear compliance damage effect ratios from a 30° sample. A damage state has been character-ized by the Cumulative Distribution Function of microcracking at that state. Estimates for the value of the CDF were made from ramp testing data using AE monitoring.

AE Results

Significant cracking, evenly distributed along the 5 cm length between sensors on 90° and off-axis samples, was detected with the AE sensors as shown in Figure 5. It is interesting to note that such cracking was not detected with the same testing apparatus in two un-toughened, more brittle materials T1000/8852 (carbon/epoxy) and S2/8852 (glass/epoxy) when tested in various off-axis directions, they displayed much less nonlinearity in their stress-strain response.
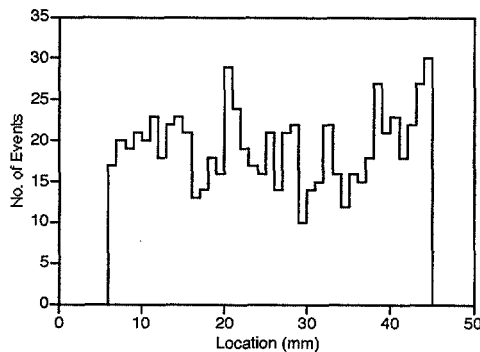
Figure 5. Histogram of cracking in the free length of a 90° sample. Events shown are between the AE sensors in a uniformly stressed portion of the material. Specimen gage length was approximately 17 cm.

Cumulative AE events detected in 90° samples tested with various stress-rates are plotted versus axial stress in Figure 6. There is no pattern with loading rate. There was significant scatter between samples in terms of the number of detectable events. Consequently, raw event counts from 90° and off-axis samples lent little insight into the rate-dependence of the microcracking.

In order to exaggerate time-dependent cracking in the 90° samples, a ramp-hold test was performed with hold periods of 20 hours. Figure 7 show cumulative events versus stress. Significant time-dependent damage is evident from the large accumulation of events during the hold periods. Possible evidence of microstructural stress relaxation is also seen during the second and third ramp periods where damage does not begin to accumulate

until the stress was increased significantly above the hold stress. Analysis of the acoustic waveforms, as discussed in (Bocchieri et.al., 2002), indicate that many similarities exist between waveforms from different sample types. Based on this evidence, events from 90° , 30° and 45° off-axis samples were analyzed identically.
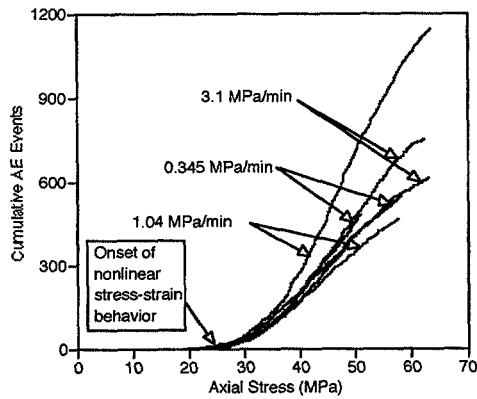

Figure 6. Cumulative AE events detected in 90° samples versus axial stress for three loading rates.
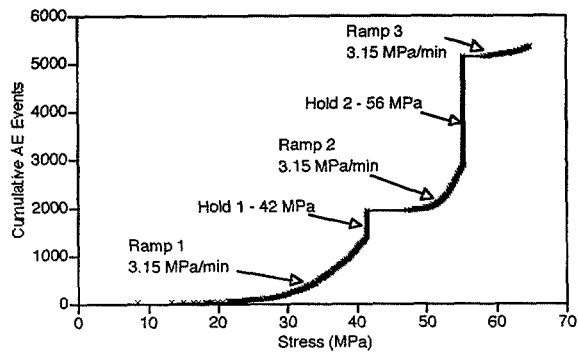

Figure 7. Cumulative AE events versus stress detected during ramp/hold testing of a 90° sample. Testing was performed with B225 sensors.

Interpretation of AE Results

Unidirectional material in its as-manufactured state contains some statistical distribution of small flaws or cracks that serve as initiation sights for crack growth (Wood and Bradley, 1997). As the composite is loaded, some of these flaws will become unstable, propagate at high speed, and stop upon reaching a crack inhibitor (fiber, reduced stress zone, etc.). If the material were elastic, each flaw would fail at a given level of globally applied stress. A histogram of the number of cracks which initiate at each stress level will therefore be common to all samples manufactured in a similar fashion. As the material is actually viscoelastic, crack initiation is a function of the time-dependent stress history. The same flaw will initiate at a lower load given sufficient time.

In this analysis, it has been assumed that *not all matrix-cracks are detected with the acoustic emission sensors.* Some microcracks arrest quickly, thus not giving off a strong acoustic wave. Others, depending on the loading, may not grow dynamically but exhibit

7

slow sub-dynamic growth. This is acceptable assuming that *a statistically significant number is detected*, yielding an accurate measure of the distribution. Testing one coupon gives the same information as cutting small specimens around a sampling of flaws and testing these individually to find the fracture stress and time.

Recognizing that not all matrix-cracks are detected with the acoustic emission sensors and that variations in the 'detectability' of events can change during a test; the *volume* of material over which cracking is detected, the *minimum size* of cracks being detected, and the *portion* of cracks detected must be held constant to obtain an accurate measure of the flaw distribution. As described in (Bocchieri, 2001)(Bocchieri et.al., 2002), changes in material acoustical properties were measured to assure the constancy of these items.

Analysis of Distributed Microcracking

Several fracture models have been developed for crack initiation and growth in nonlinear viscoelastic media [(Schapery, 1984), (Schapery, 1986)]. This theory predicts time-dependent cracking, but not the delay in cracking observed in the ramp-hold experiments due to microstructural relaxation. This type of relaxation is possible if, for example, there are separate phases of material, a softer high-stressed NLVE region near the crack tip and a stiffer linear viscoelastic (LVE) region away from the crack, each characterized by a creep compliance with different time-dependence. The toughening mechanism of rubber particles embedded in the matrix encourages this type of phenomenon as shear yielding stays localized in the vicinity of the crack tip and occurs to a much greater degree than in an unmodified epoxy (Kinloch and Hunston, 1983) (Pearson and Yee, 1983) (Shaw, 1994).

In the material studied here, high stresses near the fibers with and without existing debonds may create a phase of NLVE material in which a predominant amount of microcracking occurs. For simplicity, an idealized mechanical analog of the material is proposed containing a NLVE phase in the vicinity of crack tips (driving the crack growth) adjacent to a LVE material, as shown in Figure 8. Assuming that the NLVE phase is much softer than the linear one, stresses will redistribute to the linear phase when the global stress is held constant, thus explaining the relaxation observed from the AE data.
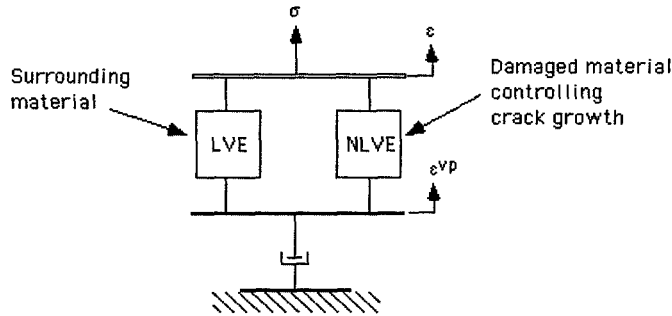
Figure 8. Idealized mechanical analog of the material containing a nonlinear viscoelastic phase in the vicinity of crack tips (driving the crack growth) surrounded by a linear viscoelastic material. A viscoplastic component has also been added to be consistent with experiments.

Implementing this idealized model and utilizing the viscoelastic fracture theory propsoed by Schapery (1984)(1986), a single combined loading parameter, L, is proposed that reflects all the major factors affecting fracture

$$L = \int_0^{t_f} \left[(\sigma_{22}^{nl})^2 + \Omega(\sigma_{12}^{nl})^2 \right]^q dt. \tag{9}$$

8

The exponent q is a constant. The stresses σ_{ij}^{nl} are the transverse and shear stresses in the NLVE phase of the model. The Ω is a time-dependent function that reflects possible changes in the viscoelastic Poisson's ratio and/or an effect of the two material phases. Stresses on each leg are found by assuming an effective linear viscoelastic relaxation modulus and viscoplastic strain. Acoustic emission testing provides the time, t_f, and stress at which each flaw fails during loading. A more complete discussion on this topic is given in (Bocchieri, 2001) and will be the subject of a forthcoming journal publication.

As L is a random variable, varying from flaw to flaw, we define $p(L)$ as the *probability mass function* , or PMF, of this variable for each specimen tested. Each sample, representative of the material, will have essentially the same mass function or distribution of initial flaws. The relative frequency, $p(L)$, of a flaw in the material of having a value of L,

$$p(L)dL = \frac{n_L}{M}dL \tag{10}$$

where $n_L dL$ is the number of flaws which grow dynamically between L and L+dL and M is the total number flaws. For our purposes we will define $n_L dL$ and M as quantities *detected* and not the actual totals in the material. Provided with an adequate sampling from the AE data, and the detectability of flaws being independent of rate, $p(L)$ will be the same.

The *cumulative distribution function* CDF,

$$P(L) = \int_0^L p(L)dL. \tag{11}$$

In physical terms, P(L) gives the proportion of flaws that have failed or run dynamically up to a given value of L. The reader is referred to (Schapery, 1974) for a similar discussion in linear viscoelastic media.

From a practical standpoint, the entire distribution of flaws will not be measurable. Each sample will fail at a different point, thus yielding only a portion of p(L) for that sample, up to say L_f. Such a distribution is said to be truncated above L_f (Benjamin and Cornell, 1970). In which case,

$$p(L) = \begin{cases} \beta p(L) & L < L_f \\ 0 & L \geq L_f \end{cases} \tag{12}$$

where

$$\beta = \frac{1}{1 - P(L_f)}. \tag{13}$$

For a given test, $P(L_f)$ is not known, so β becomes a free variable from one sample to the next.

The CDF is useful as a damage variable as it can be measured directly and does not need to be inferred from stress-strain information that may be affected by other softening mechanisms. Finally, variability in *detectable* cracks from sample to sample, which can mask differences in the time or rate effects, is easily normalized without testing a large number of specimens for each loading condition. The CDF is similar to a common damage variable, transverse crack density, used in calculating the stiffness reduction in a laminate due to transverse cracking [e.g. (Hashin, 1985)(Highsmith and Reifsnider, 1982),(Talreja, 1985)].

Measured CDF of Microcracking

Time or rate-dependence of the microcracking in 90° samples was very weak. Shown in Figure 9 is the CDF of microcracking for all monotone increasing loadings using axial stress as the distribution parameter, the parameter used if the material were simply elastic. Similar distributions were found for all loadings. The rate or time effect was only evident from ramp/hold and load/unload testing. However, use of the loading parameter, L, collapses all of the data into a single distribution as shown in Figure 10.
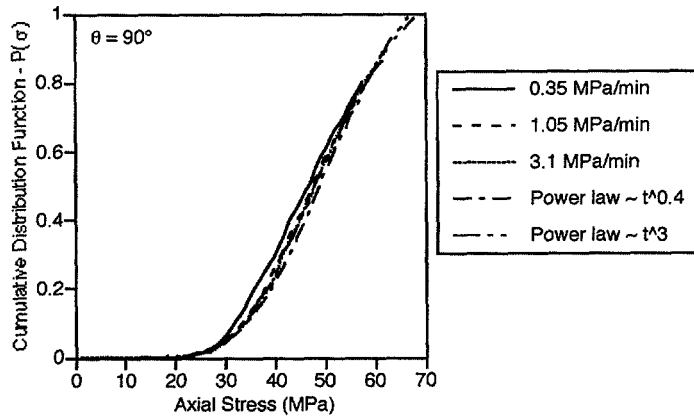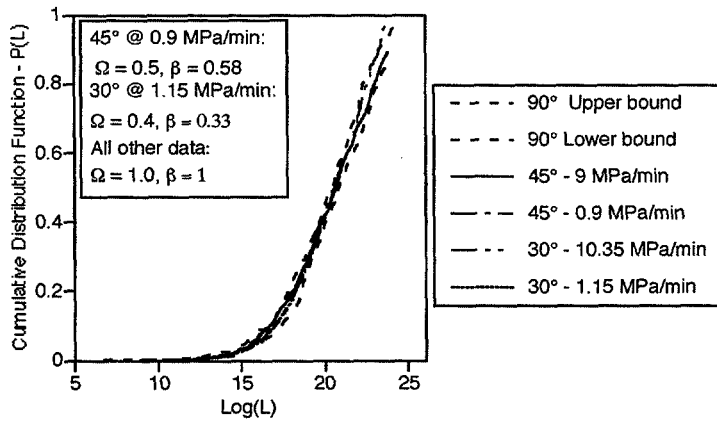
Figure 9. CDF of AE events detected from 90° samples loaded with different histories when using axial stress as the distribution parameter. Each curve represents the average of multiple cycles.
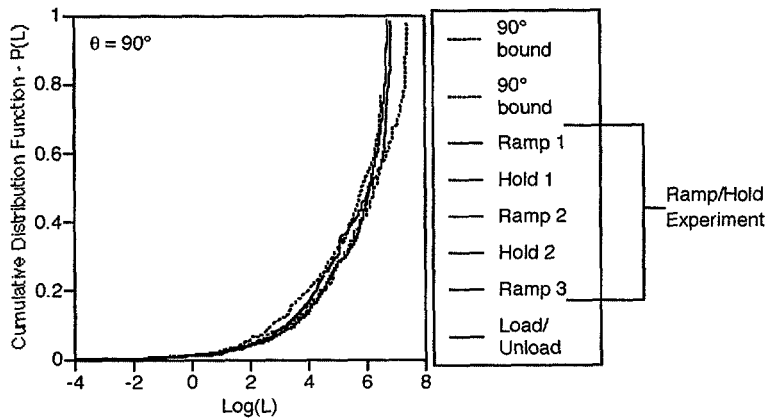
Figure 10. CDF of AE events detected from all 90° samples with L as the distribution parameter. Data bounds collected from the rate testing are shown by the dotted lines. Data from ramp/hold testing has been broken into separate pieces so cracking from each segment is easily viewed.

With the addition of shear stress, as in the off-axis samples, the rate effect on cracking becomes much stronger. However, for the rate testing performed, microstructural relaxation did not appear to be significant. As shown in Figure 11, neglecting this effect, all *high rate* testing collapses to a single distribution regardless of loading direction (also note that $\Omega=1$ so that transverse and shear stresses contribute equally to the loading parameter). At lower rates, a constant value with $\Omega < 1$, although it could be a function of time, collapses the data to a single distribution. Also note that $\beta \neq 1$ indicating that the specimens failed prior to detecting the full distribution.

Figure 11. CDF of AE events detected from off-axis and 90° samples loaded with different rates with L as the distribution parameter.

Figure legend text:
- 45° @ 0.9 MPa/min: $\Omega = 0.5$, $\beta = 0.58$
- 30° @ 1.15 MPa/min: $\Omega = 0.4$, $\beta = 0.33$
- All other data: $\Omega = 1.0$, $\beta = 1$
- Y-axis: Cumulative Distribution Function - P(L)
- X-axis: Log(L)
- --- 90° Upper bound
- --- 90° Lower bound
- —— 45° - 9 MPa/min
- —·— 45° - 0.9 MPa/min
- —··— 30° - 10.35 MPa/min
- ········ 30° - 1.15 MPa/min

Conclusion

The rubber-toughened fiber composite under study displayed significant softening effects due to nonlinear elasticity, nonlinear viscoelasticity, viscoplasticity and microstructural damage growth. Current constitutive equations that include all these mechanisms require knowledge of which material parameters are affected by damage and experimental measurement of damage growth. The *Damage Effect Study* proposed here was successful in isolating the nonlinear parameters affected by damage. The study implements vertical shifting of recovery data at different constant damage states, much like vertical shifting for the effect of stress, and requires that the parameter affecting the time scale, a_σ, is independent of damage. There was no effect of damage on this parameter in the material studied. Damage was found to only affect the transverse viscoelastic behavior through a single function, g_2^ς, regardless of fiber direction. However, two parameters were affected by damage in the viscoelastic shear strains. Finally, both the transverse and shear elastic compliances are found to stiffen with increased damage. Such a method can be used to help simplify the constitutive theory used to characterize a material and/or as a material screening process to determine whether a candidate material can be adequately characterized for a particular application.

Significant microcracking, evenly distributed along the length of all sample types, was detected by the modal acoustic emission method. An interpretation of the AE data was proposed based on an initial population of existing flaws. Then a cumulative distribution function of microcracking was defined and used to study effects of stress history. Time or rate-dependence of the microcracking in 90° samples was very weak and only evident from ramp-hold and load-unload testing. With the addition of shear stress, as in the off-axis samples, the rate effect became stronger. Ramp-hold testing provided evidence of microstructural stress relaxation which lead to an idealized 2-phase material model consisting of linear and nonlinear viscoelastic phases. Then a single loading parameter, which is derived from viscoelastic fracture mechanics, was proposed. Using this model, a single damage distribution parameter was found independent of loading history for the 90° samples, thus supporting the theory. A simplified analysis of data from off-axis testing collapse data from all samples and loading histories. With this loading parameter, the damage state (as a percentage of the microcrack density at failure) resulting from constant rate, load-unload and ramp-hold loadings can be predicted.

Acknowledgement

References

Abdel-Tawab, K. and Y. Weitsman: 1998, 'A Coupled Viscoelasticity/Damage Model with Application to Swirl-Mat Composites'. *Int. Journal of Damage Mechanics* **7**, 351–380.

Benjamin, J. and C. Cornell: 1970, *Probability, Statistics, and Decision for Civil Engineers*. McGraw-Hill Book Company.

Bocchieri, R.: 2001, 'Time-Dependent Deformation of a Nonlinear Viscoelastic Rubber-toughened Fiber Composite with Growing Damage'. Ph.D. thesis, The University of Texas at Austin.

Bocchieri, R. and R. Schapery: 2000, 'Nonlinear Viscoelastic Behavior of Rubber-toughened Carbond and Glass/Epoxy Composites'. In: R. Schapery and C. Sun (eds.): *Time Dependent and Nonliear Effects in Polymers and Composites, ASTM STP 1357*. American Society for Testing and Materials, pp. 238–265.

Bocchieri, R., R. Schapery and M. Gorman: 2002, 'Time-dependent Microcracking Detected in a Rubber-toughened Carbon/Epoxy Composite by the Modal Acoustic Emission Method'. *(submitted to the J. of Comp. Matls)*.

Ha, K. and R. Schapery: 1997, 'A Three-Dimensional Viscoelastic Constitutive Model for Particulate Composites with Growing Damage and its Experimental Validation'. *Int. J. Solids Struc.* **35**, 3497–3517.

Hashin, Z.: 1985, 'Analysis of Cracked Laminates: A Variational Approach'. *Mech. of Matls* **4**, 121–136.

Hashin, Z. and Z. Rotem: 1978, 'Cumulative Damage Theory of Fatigue Failure'. *Matl's Sci. and Eng.* **34**.

Highsmith, A. and K. Reifsnider: 1982, 'Stiffness Reduction Mechanisms in Composite Laminates'. In: K. Reifsnider (ed.): *Damage in Composite Materials, ASTM STP 775*. American Soc. for Testing Materials, pp. 103–117.

Kinloch, A.J., S. S. and D. Hunston: 1983, 'Deformation and Fracture Behavior of a Rubber-Toughened Epoxy: 2. Failure Criteria'. *Polymer* **24**, 1355.

Park, S. and R. Schapery: 1997, 'A Viscoelastic Consitutitive Model for Particulate Composites with Growing Damage'. *Int. J. Solids and Struc.* **34**, 931–947.

Pearson, R. and A. Yee: 1983, 'Effect on Crosslink Density on the Toughening Mechanism of Elastomer Modified Epoxies'. *Polym. Mater. Sci. Eng.* **49**, 316–.

Schapery, R.: 1969, 'On the Characterization of Nonlinear Viscoelastic Materials'. *Polymer Eng. Sci.* **9**, 295–310.

Schapery, R.: 1974, 'A Nonlinear Constitutive Theory for Particulate Composites Based on Viscoelastic Fracture Mechanics'. In: *JANNAF Structures and Mechanical Behavior Working Group.*

Schapery, R.: 1984, 'Correspondence principles and a generalized J integral for large deformation and fracture analysis of viscoelastic media'. *Int. J. of Fract.* **25**, 195–223.

Schapery, R.: 1986, 'Time-Dependent Fracture: Continuum Aspects of Crack Growth'. In: M. Bever (ed.): *Encyclopedia of Materials Science and Engineering*. Pergamon Press, pp. 5043–5053.

Schapery, R.: 1987, 'Deformation and fracture characterization of inelastic composite materials using potentials'. *Polymer Eng.and Sci.* **27**, 63–76.

Schapery, R.: 1990a, 'On some path independent integrals and their use in fracture of nonlinear viscoelastic media'. *Int. J. of Fract.* **42**, 189–207.

Schapery, R.: 1990b, 'A theory of mechanical behavior of elastic media with growing damage and other changes in structure'. *J. Mech. Phys. Solids* **38**, 215–253.

Schapery, R.: 1999, 'Nonlinear viscoelastic and viscoplastic constitutive equations with growing damage'. *Int. J. of Fract.* **97**, 33–66.

Shaw, S.: 1994, 'Rubber modified epoxy resins'. In: A. Collyer (ed.): *Rubber Toughened Engineering Plastics*. Chapman & Hall, pp. 165–209.

Talreja, R.: 1985, 'Transverse Cracking and Stiffness Reduction in Composite Laminates'. *J. Comp. Matls* **19**, 355–375.

Wood, C. and W. Bradley: 1997, 'Determination of the Effect of Seawater on the Interfacial Strength of an Interlayer E-glass/Graphite/Epoxy Composite by In Situ Observation of Transverse Cracking in an Environmental SEM'. *Comp. Sci. Tech.* **57**, 1033–1043.